

# Magnetic excitations in the ordered phases of praseodymium hexaboride

M D Le<sup>1</sup>, K A McEwen<sup>1</sup>, J-G Park<sup>2</sup>, S Lee<sup>2</sup>, F Iga<sup>3</sup> and K C Rule<sup>4</sup>

<sup>1</sup> Department of Physics and Astronomy, and London Centre for Nanotechnology, University College London, Gower Street, London, WC1E 6BT, UK

<sup>2</sup> Department of Physics and Institute of Basic Science, SungKyunKwan University, Suwon 440-746, Korea

<sup>3</sup> Department of Quantum Matter, School of Advanced Sciences of Matter, Hiroshima University, Higashi-Hiroshima 739-8526, Japan

<sup>4</sup> Berlin Neutron Scattering Centre, Hahn-Meitner-Institut, Glienicker Strasse 100, Berlin D-14109, Germany

## Abstract.

We have made the first inelastic neutron scattering measurements on single crystal PrB<sub>6</sub>, studying the magnetic excitations in the ordered phases. The lowest energy mode has a minimum energy of  $\approx 1.0$  meV at the magnetic zone centre, with a significant dispersion along the [001] direction, but very little dispersion along [110]. Interactions out to fourth nearest neighbours are required to explain the [001] dispersion. Measurements of the temperature dependence of the excitations show a strong softening and broadening of the lowest energy mode at the magnetic zone centre between 2K (commensurate phase) and 5K (incommensurate phase).

PACS numbers: 78.70.Nx, 75.30.Ds

Submitted to: *J. Phys.: Condens. Matter*

## 1. Introduction

The rare-earth hexaborides have the cubic CaB<sub>6</sub> structure (space group  $Pm\bar{3}m$ ), with rare-earth ions lying on a simple cubic lattice enclosing an octahedral B<sub>6</sub> cage. The RB<sub>6</sub> compounds show many interesting magnetic and electronic properties. For example, the much studied compound SmB<sub>6</sub> exhibits mixed valence behaviour [1, 2] whilst CeB<sub>6</sub> shows quadrupolar ordering [3, 4]. The remaining compounds are either antiferromagnetic metals or ferromagnetic semiconductors, depending on whether the rare-earth ion is trivalent or divalent respectively [5].

PrB<sub>6</sub>, with lattice parameter  $a = 4.13$  Å, falls into the former category. It exhibits two phase transitions, (i) at  $T_N = 7$ K to an incommensurate (IC) antiferromagnetic (AFM) phase with wave vector  $\mathbf{q}_1 = (1/4 - \delta, 1/4, 1/2)$  where  $\delta \approx 0.05$ , and (ii) at  $T_2$

= 4.2K to a commensurate (C) AFM phase with  $\mathbf{q}_2 = (1/4, 1/4, 1/2)$  [6]. The magnetic structure in each phase is shown in figure 1a.

Earlier inelastic neutron scattering work on polycrystalline PrB<sub>6</sub> revealed the crystal field splitting of the Hund's rules  $J = 4$  ground multiplet of the Pr<sup>3+</sup> ion [7]. At low temperatures, Loewenhaupt and Prager measured transitions from the ground state with energies 27 meV and 32 meV. At T = 250 K, they measured transitions with energies between 5-8 meV from the excited states. From these results they deduced the Lea, Leask and Wolf (LLW) [8] crystal field parameters as  $x = 0.95$  and  $W = 9.5$  K = 0.82 meV. These parameters give a  $\Gamma_5$  triplet ground state, with a  $\Gamma_3$  doublet at 27 meV, a  $\Gamma_4$  triplet at 32 meV and a  $\Gamma_1$  singlet at 39 meV.

The high temperature magnetic susceptibility [9] yields an effective paramagnetic moment of  $3.7 \mu_B$  per Pr atom, a paramagnetic Curie temperature of -36 K, and is well described by these crystal field parameters. However, below  $\approx 80$  K, the measured susceptibility is greater than the calculated crystal field susceptibility, whilst at  $\approx 20$  K the measured values decrease slightly before a sharp decrease at  $T_N$ . This initial decrease has been attributed to short range antiferromagnetic ordering above  $T_N$  [9] which is in accord with <sup>11</sup>B NMR [10] and thermal conductivity [11] studies. In addition the entropy change at  $T_N$  from heat capacity measurements is  $5.1 \text{ JK}^{-1}\text{mol}^{-1}$ , less than the expected  $R\ln(3)=9.1 \text{ JK}^{-1}\text{mol}^{-1}$  value of a triplet ground state, which further supports the hypothesis of short range ordering.

Finally, the measured ordered moment of  $1.2 \mu_B$  per Pr atom is less than the  $2.0 \mu_B$  per Pr atom expected from the  $\Gamma_5$  triplet ground state. This reduction has been attributed to the coexistence of antiferroquadrupolar (AFQ) ordering together with the AFM ordering [9]. This is further supported by the magnetic structure in the C phase where the moments are in the  $\langle 110 \rangle$  directions, as this easy direction is selected if there is a coexistence of an  $O_{xy}$  AFQ ordering with the AFM. Other AFQ order parameters are ruled out by the presence of a triplet ground state.

In the ordered phase, the molecular field will split the ground state triplet into three singlets. Thus, any low energy magnetic excitations will come from transitions between these levels, as the excited crystal field states are so much higher in energy that they will perturb the triplet relatively little. We have measured these low energy excitations in the two ordered phases of PrB<sub>6</sub>, and report their dispersion and temperature dependence in the present paper.

## 2. Experimental Details

The inelastic neutron scattering measurements were performed on the V2-Flex triple axis spectrometer at the BER-II reactor of the Berlin Neutron Scattering Centre, Hahn-Meitner-Institut, Berlin. A single crystal of PrB<sub>6</sub> was grown by a travelling solvent floating zone method using a mirror furnace equipped with Xe lamps at Hiroshima University. In order to avoid the high neutron absorption of natural boron, we used boron with 99% of the low absorption <sup>11</sup>B in our starting material. For this experiment

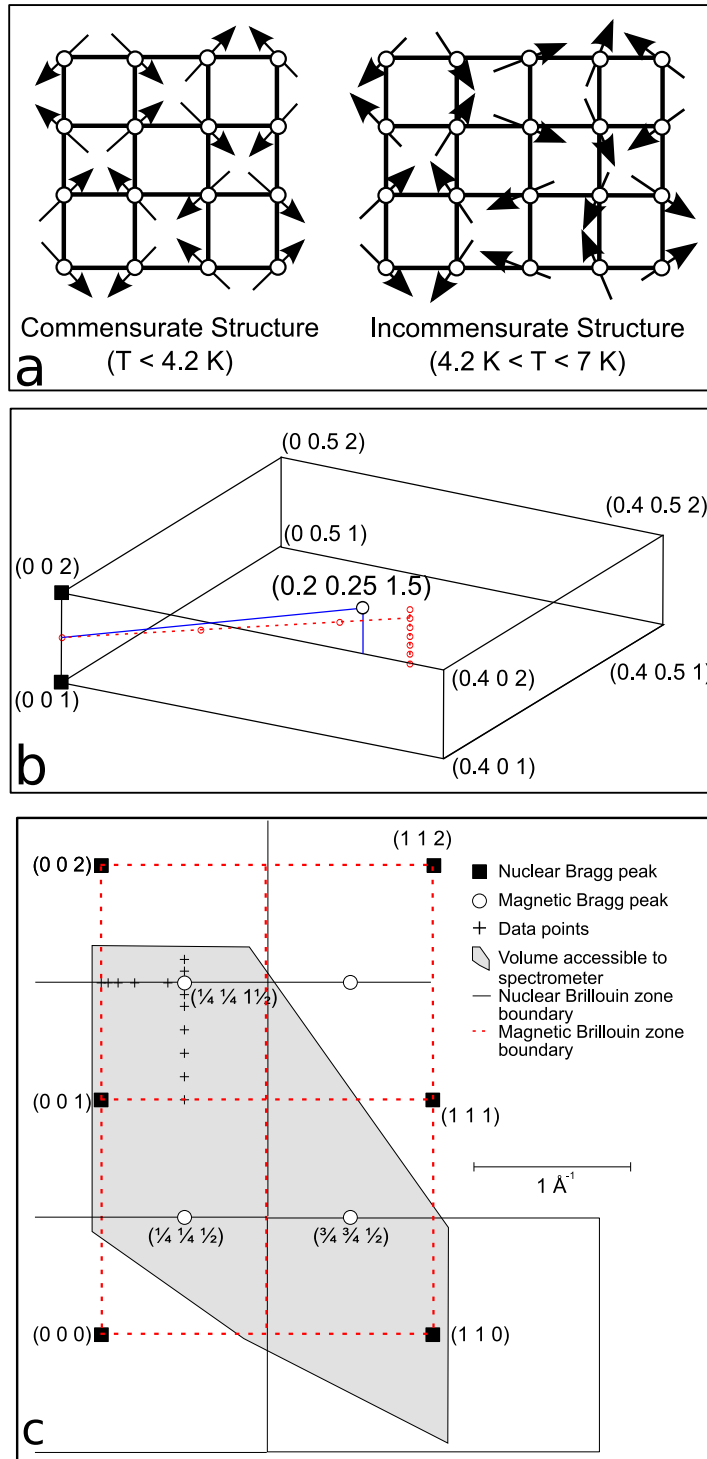


**Figure 1.** *Magnetic structure and reciprocal space diagram.* **Panel a)** shows the magnetic structure in the commensurate and incommensurate phases. **Panel b)** shows the magnetic Brillouin zone in the incommensurate phase at 5 K. The blue solid lines indicate the major symmetry directions, whilst the red dashed lines and open circles show the wavevectors at which data were taken. Note that the horizontal scales have been exaggerated to emphasize the difference between the high symmetry and data directions. **Panel c)** shows the scattering plane in the commensurate phase at 2 K, with the nuclear and magnetic Brillouin zones and wavevectors where data were taken.

we cut a sample of dimension of  $5 \times 5 \times 30 \text{ mm}^3$  with faces parallel to the (0 0 1) and (1 1 0) planes. It was mounted in an Orange cryostat with the [0 0 1] and [1 1 0] directions defining the horizontal scattering plane.

The spectrometer was operated with fixed final wavevector,  $k_f = 1.55 \text{ \AA}^{-1}$  using PG(002) crystals for both the monochromator and analyser. 60' collimators were installed between the monochromator, sample, analyser and detector as appropriate to reduce the background, and a Be filter was installed between the sample and analyser to reduce higher order contamination. In this configuration the experimental resolution, measured with a Vanadium sample, was 0.14 meV at zero energy transfer, and calculated to be 0.17 and 0.19 meV at  $\Delta E = 1.0$  and 2.0 meV, respectively.

Scans were made at 10, 5, 3.8 and 2 K, with energy transfers up to 5 meV. Typical counting times were approximately 15-20 min per point. We chose to investigate the excitations in the magnetic Brillouin zone centred at  $(1/4 \ 1/4 \ 3/2)$ , with measurements in the [1 1 0] and [0 0 1] directions, as shown in figure 1.

### 3. Experimental Results

Figures 2a and 3a show scans at constant wavevector transfer in the commensurate phase of  $\text{PrB}_6$  at 2 K. The scans have been fitted with Gaussian peaks which are shown as solid lines in the plots. As seen in figure 2a, we observed three modes at the magnetic zone edge at wavevector transfer  $\mathbf{Q}=(0 \ 0 \ 3/2)$ , two of which merge into one going along  $[h \ h \ 3/2]$  towards the magnetic zone centre  $\mathbf{Q}=(1/4 \ 1/4 \ 3/2)$ . The higher energy mode, centred at  $\approx 1.9$  meV energy transfer, showed little dispersion, and a fairly constant resolution limited width ( $\approx 0.2$  meV) and intensity ( $\approx 35$  counts/ $4 \times 10^6$  monitor counts in the peak). The two lower energy modes show a modest dispersion before they merge at  $\mathbf{Q} \approx (0.15 \ 0.15 \ 3/2)$ . The combined intensity of the two modes remains approximately constant, as do their widths. The broad peak seen at  $\mathbf{Q}=(0.1 \ 0.1 \ 3/2)$  and  $\mathbf{Q}=(0.2 \ 0.2 \ 3/2)$  shows that the two low energy modes, whilst not separately resolved in the data, have not yet merged entirely. In contrast, at  $\mathbf{Q}=(1/4 \ 1/4 \ 3/2)$  we see a resolution limited peak whose width, 0.21 meV, is comparable to those of the peaks at  $\mathbf{Q}=(0 \ 0 \ 3/2)$  which vary from 0.21 to 0.24 meV.

Along the [0 0 1] direction, in contrast, we observed a very dispersive mode with energy from  $\approx 1.0$  meV at the magnetic zone centre to  $\approx 2.1$  meV at the zone boundary (see figure 3a). In addition, around the zone centre we also observed another mode 1 meV higher in energy, with approximately one third the intensity of the lower energy mode. As is apparent from figure 3a, this higher energy mode appears to show an asymmetric dispersion about the magnetic zone centre. However, the peak at  $\mathbf{Q}=(1/4 \ 1/4 \ 1.45)$  is much broader than the corresponding peaks at  $(1/4 \ 1/4 \ 1.5)$  or  $(1/4 \ 1/4 \ 1.55)$ , but with similar peak intensity. This anomaly will need further investigation.

Figures 2b and 3b show scans in the incommensurate phase at 5 K. Unfortunately because of the orientation of the sample and cryostat, we were unable to tilt far enough to access wavevectors along the high symmetry directions in the incommensurate phase,

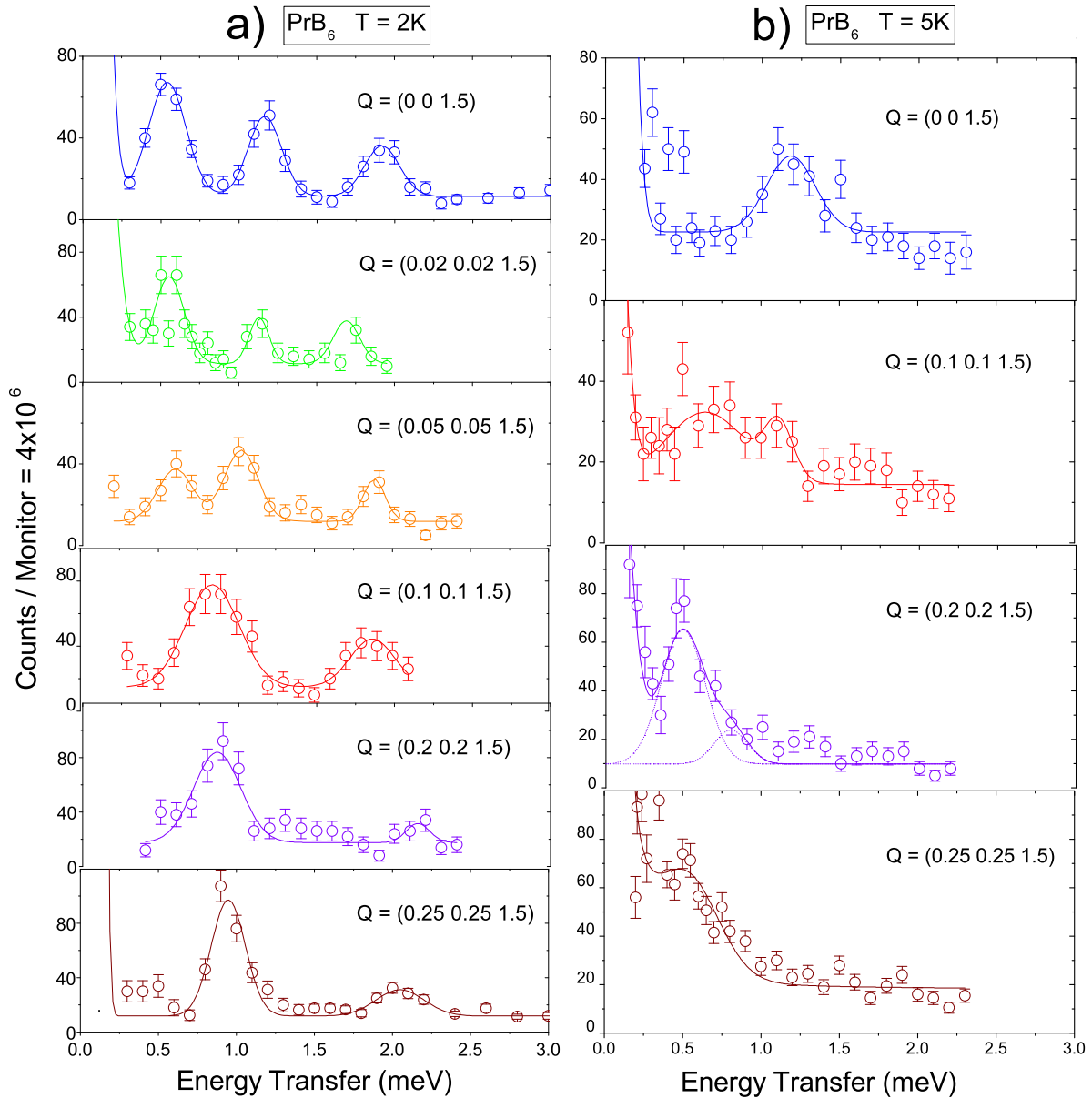


**Figure 2.** Scans along  $[h h 3/2]$ . The left panel shows scans at 2 K in the commensurate phase, whilst the right panel shows scans at 5 K in the incommensurate phase. The solid lines are Gaussian fits to the data.

i.e. along  $\mathbf{Q}=(0.2 0.25 1)$  or  $\mathbf{Q}=(h 5/4h 3/2)$ . The wavevectors at which data were taken, and for comparison, the high symmetry directions, are marked in figure 1b.

In contrast to the shape of the dispersion of the excitations along  $[h h 3/2]$  in the C phase, in the IC phase, as shown in figure 2b, the modes have a minimum of 0.6 meV at  $\mathbf{Q}=(1/4 1/4 3/2)$ , the C phase magnetic zone centre, and a maximum of 1.3 meV at the magnetic zone boundary,  $\mathbf{Q}=(0 0 3/2)$ . In between these two end points, we observed a broad range of scattering at  $\mathbf{Q}=(0.1 0.1 3/2)$  which we have interpreted to be two modes that are just resolved. The second, higher energy, mode may also be seen

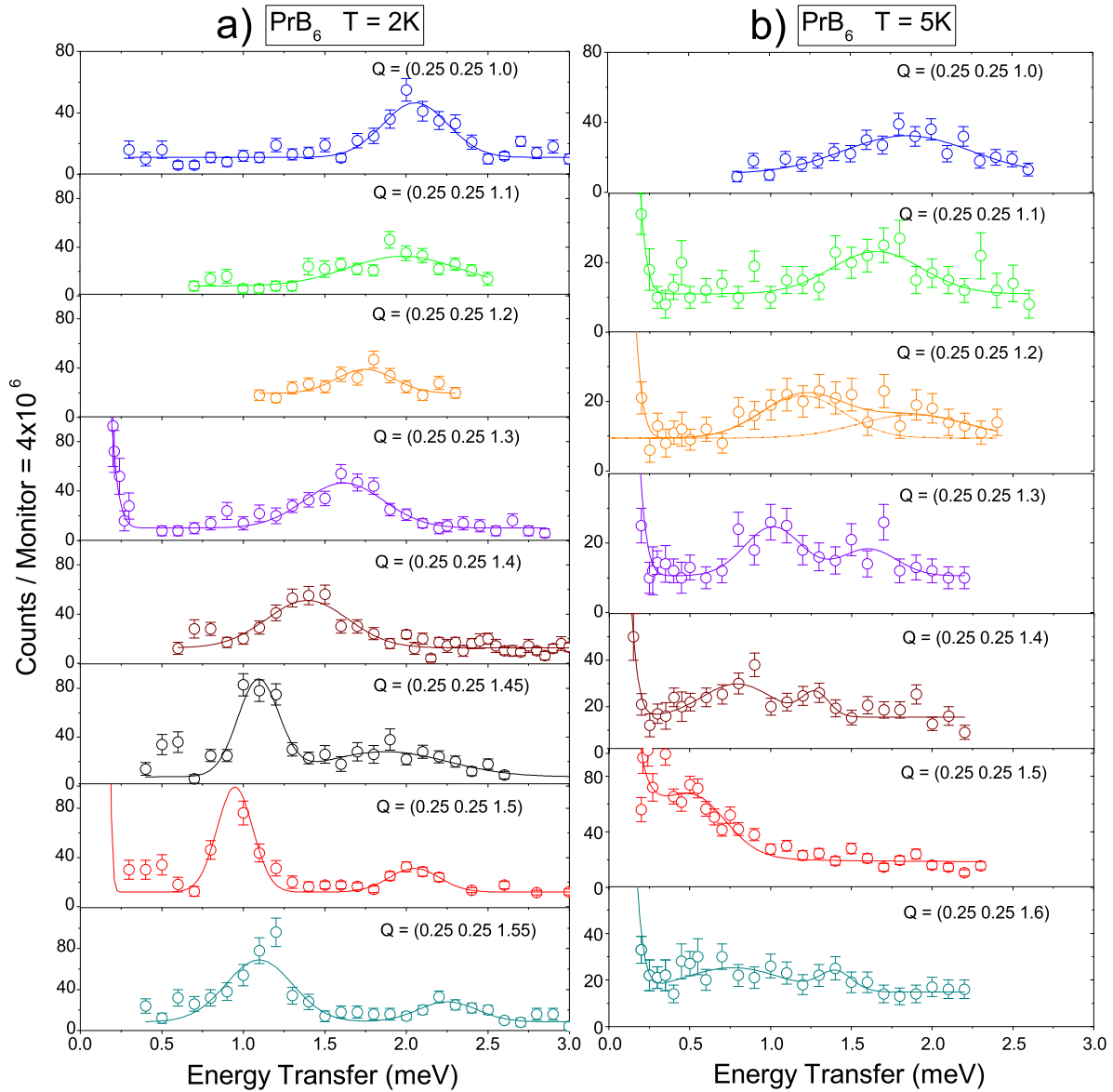


**Figure 3.** Scans along  $[1/4 \ 1/4 \ l]$ . The left panel shows scans at 2 K in the commensurate phase, whilst the right panel shows scans at 5 K in the incommensurate phase. The solid lines are Gaussian fits to the data.

at  $\mathbf{Q}=(0.2 \ 0.2 \ 3/2)$  as a shoulder to the higher intensity low energy peak.

The dispersive modes along  $[1/4 \ 1/4 \ l]$  observed in the C phase were again seen in the IC phase, shown in figure 3b. However, in this phase we observed two modes across most of the magnetic Brillouin zone, separated in energy by  $\approx 0.5$  meV. The lower energy mode is softened by  $\approx 0.5$  meV with respect to the mode observed in the C phase at 2 K. The peaks in this phase were much broader than in the C phase, with  $\text{FWHM} \approx 0.4$  meV, so it was difficult to resolve some of them. We note that, at  $\mathbf{Q}=(1/4 \ 1/4 \ 3/2)$ , the C phase magnetic zone centre, there appears to be only a single excitation at 0.53 meV. This corresponds to the minimum energy of the lower mode, whilst the intensity of the

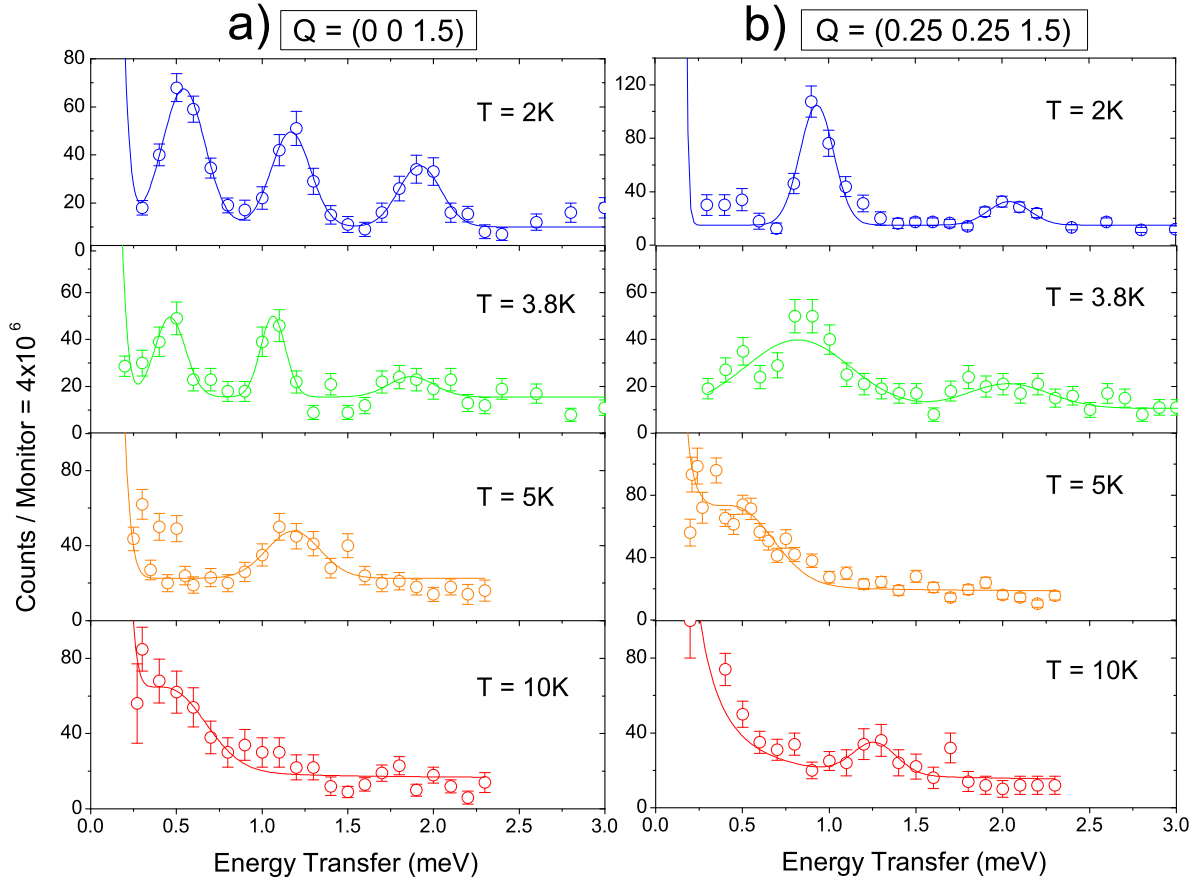


**Figure 4.** *Temperature dependence of the inelastic spectra.* a) shows spectra from the magnetic Brillouin zone edge and b) shows spectra from the zone centre. The solid lines are fits using Gaussians for the inelastic peaks and Gaussian or a pseudo-Voigt function for the elastic line.

upper mode has apparently vanished.

Finally, figure 4 shows scans at the magnetic Brillouin zone edge, at  $\mathbf{Q}=(0\ 0\ 3/2)$ , and zone centre, at  $\mathbf{Q}=(1/4\ 1/4\ 3/2)$ , measured at 2 K and 3.8 K in the C phase, at 5 K in the IC phase, and at 10K in the paramagnetic phase. The inelastic peaks and the elastic peaks in the C and IC phases were fitted with Gaussian peaks, but the quasielastic broadening in the paramagnetic phase was fitted using a pseudo-Voigt function with both Gaussian and Lorentzian components having the same widths and centred on zero energy transfer. We observed that the three modes in the C phase at the magnetic zone edge appear to become one mode in the IC phase, and that there is a steady decrease of intensity with increasing temperature which is in accord with the reduction in the thermal occupation of the ground state. A similar reduction in intensity was observed at the magnetic zone centre, where we also saw that the two modes in the C phase become a single mode in the IC phase, although as noted above from the dispersion of the modes along  $[0\ 0\ 1]$  we should expect two peaks at this wavevector in the IC phase also.

We also observed a small inelastic peak in the paramagnetic phase, centred at 1.25 meV at the magnetic zone centre, which appears to be softened to around 0.5 meV at the magnetic zone edge. This peak may arise from short range AFM ordering as observed in bulk measurements noted in section 1.

#### 4. Discussion

$\text{Pr}^{3+}$  has total angular momentum number  $J = 4$  in accord with Hund's rules. Thus the ground state  $\Gamma_5$  triplet has wavefunctions  $\psi_1 = \beta|3\rangle - \alpha|-1\rangle$ ,  $\psi_2 = \frac{1}{\sqrt{2}}\{|2\rangle - |-2\rangle\}$ ,  $\psi_3 = \beta|-3\rangle - \alpha|1\rangle$  due to the crystal field splitting, with  $\alpha=0.354$ ,  $\beta=0.935$ . When a molecular field splits this triplet,  $\psi_1$  becomes the new ground state singlet, with energy  $\Delta$  between  $\psi_1$  and  $\psi_2$  and  $2\Delta$  between  $\psi_1$  and  $\psi_3$ . Thus the only dipolar transition from the ground state  $\psi_1$  is  $\psi_1 \rightarrow \psi_2$ . However, when the field-induced mixing of the higher excited crystal field states into the new ground state is taken into account there is a small dipole matrix element between  $\psi_1$  and  $\psi_3$ . This is negligible unless the molecular field is very strong, giving rise to a large  $\Delta$ . For the observed energies of the modes, in the range 0.5 - 2.0 meV, this mixing gives a matrix element between  $\psi_1$  and  $\psi_3$  which is less than 1% of the value of that between  $\psi_1$  and  $\psi_2$ .

In addition, at 2 K, for the observed range of  $\Delta$  we should expect only the ground state to be thermally occupied, and hence only a single excitation per magnetic Pr site. However, even at 5 K where there is some thermal occupation of the excited  $\psi_2$  level, we should still expect to see one excitation per Pr site, as the splitting between  $\psi_1$  and  $\psi_2$  and between  $\psi_2$  and  $\psi_3$  are the same.

As the magnetic unit cell is twice the nuclear unit cell in the C phase in both the  $[\text{h h } 3/2]$  and  $[1/4 \ 1/4 \ 1]$  directions, we should expect to see a maximum of four modes arising from the  $\psi_1 \rightarrow \psi_2$  transition. Some of these may, of course, be degenerate. The situation will be further complicated by the likely existence of multiple domains in the sample. In the C phase, we have observed only three modes along the  $[\text{h h } 0]$  direction and two along the  $[0 \ 0 \ 1]$  direction. Although we have taken data up to 5 meV energy transfer, no further excitations were detected. It may be that the intensity of any higher energy modes is too low to be observed.

Figure 5 shows the dispersion of the modes along the  $[1/4 \ 1/4 \ 1]$  and  $[\text{h h } 3/2]$  directions (left and right panels respectively) in both the C and IC phases (top and bottom respectively). The points plotted are the peaks of Gaussians fitted to the data, and the error bars indicate the calculated errors on the peak positions from the fits. The dispersion along the  $[1/4 \ 1/4 \ 1]$  directions was fitted to a model for dispersive magnetic excitations arising from crystal field transitions [12]:

$$E(\mathbf{Q}) = \sqrt{\Delta \{\Delta - 2n_{01}M^2J_{zz}(\mathbf{Q})\}} \quad (1)$$

where  $\Delta$  is the CF splitting,  $M^2 = |\langle\psi_2|J^\pm|\psi_1\rangle|^2$  is the matrix element between the ground and excited states, and  $n_{01} = 1 - \exp(-\Delta/k_B T)$  is the difference in population between these two states. Taking  $M^2 = 3.2$  from the crystal field wavefunctions in a

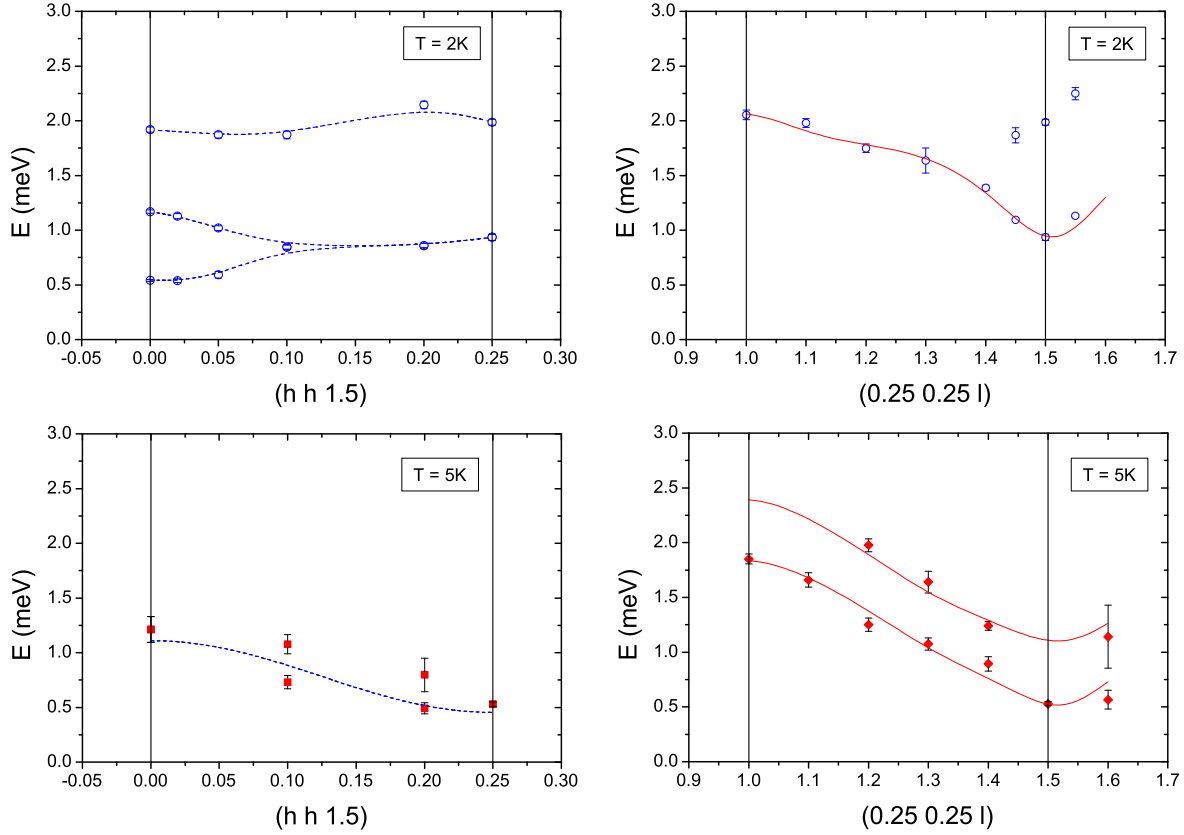


**Figure 5.** Dispersion relations at 2 K and 5 K. The full red lines are fits as described in the text, the dashed blue lines are guides to the eye. The points represent the fitted peak positions.

molecular field of 15 T which gives  $\Delta = 1.6$  meV, we found a good fit by including up to fourth nearest neighbour interactions with:

$$J_{zz}(\mathbf{q}) = \sum_{n=1}^4 J_n \cos(2n\pi q_l a) \quad (2)$$

The fitted parameters are shown in Table 1. The two modes in the IC phase were fitted simultaneously using the same  $J_n$  values with different  $\Delta$  for each mode. In the C phase, however only the lower energy mode was fitted due to the lack of data points for the higher energy modes.

In conclusion, we have measured the dispersion of crystal field excitations between the split triplet ground state of  $\text{Pr}^{3+}$  in  $\text{PrB}_6$ . These show strong dispersion along the  $[0\ 0\ l]$  direction, with a width of 1 meV, but less dispersion along the  $[h\ h\ 0]$  direction. Further measurements in a magnetic field and theoretical calculations are in progress.

C Phase (2K)				IC Phase (5K)			
$\Delta$	=	1.66	$\pm$ 0.06	$\Delta_1$	=	1.28	$\pm$ 0.06
				$\Delta_2$	=	1.79	$\pm$ 0.11
$J_1$	=	-0.13	$\pm$ 0.02	$J_1$	=	-0.19	$\pm$ 0.02
$J_2$	=	0.020	$\pm$ 0.02	$J_2$	=	-0.024	$\pm$ 0.02
$J_3$	=	-0.032	$\pm$ 0.02	$J_3$	=	-0.013	$\pm$ 0.02
$J_4$	=	0.009	$\pm$ 0.01	$J_4$	=	0.005	$\pm$ 0.03

**Table 1.** Parameters fitted from dispersion relation, in meV. See text for details

## Acknowledgments

We thank Jens Jensen and Michael Loewenhaupt for valuable discussions. MDL thanks EPSRC for the provision of a research studentship. This research project has been supported by the European Commission under the 6th Framework Programme through the Key Action: Strengthening the European Research Area, Research Infrastructures. Contract number RII3-CT-2003-505925 (NMI3). Work at Sungkyunkwan University was supported by the Korea Research Foundation (Grant No. 2005-C00153), the BAERI program, and the LG Yonam Foundation.

## References

- [1] Vanstein E E, Blokhin S M, and Paderno Yu B 1965 *Sov. Phys. Solid State* **6** 281
- [2] Alekseev P A, Mignot J-M, Rossat-Mignod J, Lazukov V N, Sadikov I P, Konovalova E S, and Paderno Yu B 1995 *J. Phys.: Condens. Matter.* **7** 289
- [3] Yakhou F, Plakhty V, Suzukic H, Gavrilov S, Burlet P, Paolasini L, Vettier C, and Kunii S 2001 *Phys. Lett. A* **285** 191
- [4] Nakao H, Magishi K, Wakabayashi Y, Murakami Y, Koyama K, Hirota K, Endoh Y, and Kunii S 2001 *J. Phys. Soc. Jap.* **70** 1857
- [5] Geballe T H, Matthias B T, Andres K, Maita J P, Cooper A S, and Corenzwit E 1968 *Science* **160** 1443
- [6] Burlet P, Effantin J M, Rossat-Mignod J, Kunii S, and Kasuya T 1988 *J. Phys. (Paris) C* **8** 459
- [7] Loewenhaupt M, and Prager M 1986 *Z. Phys. B* **62** 195
- [8] Lea K R, Leask M J M, and Wolf W P 1962 *J. Phys. Chem. Solids* **23** 1381
- [9] Kobayashi S, Sera M, Hiroi M, Nishizaki T, Kobayashi N, and Kunii S 2001 *J. Phys. Soc. Jap.* **70** 1721
- [10] Takagi S, Itabashi S, Kunii S, and Kasuya T 1985 *J. Mag. Mag. Mat.* **51** 267
- [11] Sera M, Kobayashi S, Hiroi M, and Kobayashi N 1996 *Phys. Rev. B* **54** R5207
- [12] Jensen J, and Mackintosh A R, 1991 *Rare Earth Magnetism* (Oxford: Clarendon Press)